CrossMark

Synthesis and xanthine oxidase inhibitory activity of 5,6-dihydropyrazolo/pyrazolo[1,5-c]quinazoline derivatives

Deependra Kumar [a], Gagandeep Kaur [a], Arvind Negi [a], Sanjeev Kumar [b], Sandeep Singh [c], Raj Kumar [a],*,1

[a] Laboratory for Drug Design and Synthesis, Centre for Chemical and Pharmaceutical Sciences, School of Basic and Applied Sciences, Central University of Punjab, Bathinda 151 001, India
[b] Centre for Biosciences, School of Basic and Applied Sciences, Central University of Punjab, Bathinda 151 001, India
[c] Centre for Genetic Diseases and Molecular Medicine, Central University of Punjab, Bathinda 151 001, India

ARTICLE INFO

ABSTRACT

Some 5,6-dihydropyrazolo/pyrazolo[1,5-c]quinazoline derivatives were rationally designed, synthesized and evaluated for *in vitro* xanthine oxidase inhibitory activity for the first time. Some notions about structure activity relationships are presented. The compounds **6g**, **6h** and **6e** were found to be significantly active against XO. The compound **6g** emerged as the most potent XO inhibitor as compared to allopurinol and free radical scavenger. The molecular docking of **6g** into the XO active site highlighted its mode of binding and important interactions such as hydrogen bonding, π–π stacking with amino acid residues like Ser876, Thr1010, Phen914, Phe1009 and Phe649 and its close proximity to dioxothiomolybdenum (MOS).

1. Introduction

Xanthine oxidase (XO; EC 1.17.3.2) is well characterized druggable target [1–3] for the treatment and management of disease conditions involving high uric acid level; hyperuricemia and gout [4,5] due its significant role in catalytic oxidative hydroxylation of hypoxanthine and xanthine to produce uric acid. Further XO is also associated and unregulated in pathological conditions involving inflammation, metabolic disorders, cellular aging, reperfusion damage, atherosclerosis, hypertension [6,7] and carcinogenesis as it generates superoxide anions, H_2O_2 and highly reactive species (ROS) during the catalytic process [2]. Thus the selective inhibition of XO may result in broad spectrum therapeutics for gout, cancer, inflammation and oxidative damage [2–4].

In general XO inhibitors have been classified into purine and non-purines based on their scaffolds mimicking to naturally occurring purines (Fig. 1). Allopurinol (**1**) was the first purine based XO inhibitor approved by the US FDA in 1966 for treatment of gout and hyperuricemia [8]. Due to the reported hypersensitivity (Stevens–Johnsons) syndrome induced by allopurinol use [9,10], researchers initiated their search for new XO inhibitors derived non-purine skeleton [4,11–16] and a great success has been achieved in this direction which is evident by a recent US FDA approval of

febuxostat [17] (**2**) having lesser and non-life threatening side effects as compared to allopurinol [18–20].

In continuation to our earlier successful attempts made towards the search for new xanthine oxidase inhibitors based on N-(1,3-diaryl-3-oxopropyl)amides [11] (**3**) and N-acetyl pyrazolines [12] (**4**), we thought of designing and synthesizing 5,6-dihydro pyrazolo[1,5-c]quinazolines (**5** and **6**) *via* structural modification of **3**, **4** and FYX-051 keeping in mind the following considerations (Fig. 2): (i) two aryl/heteroaryl rings (preferably joined by three atoms) oriented in such a way so that favorable arene–arene interactions with Phe914 and Phe1009 amino acid residues may take place; (ii) a site for hydroxylation near molybdenum metal and (iii) bioisosteric replacement of free C=O with C=N/C−NH followed by ring cyclization might enhance activity and target specificity through hydrogen bond formation with Ser876 and/or Thr1010 amino acid residues of XO active site.

Pyrazolo[1,5-c]quinazolines have previously been reported to possess bioactivities such as benzodiazepine binding ligands [21], Gly/NMDA receptor, excitatory amino acid antagonists [22,23], IKK [24], phosphodiesterase 10A [25] inhibitors, AMPA and kainate receptor antagonists [26] and adenosine receptor antagonists [27].

2. Materials and methods

2.1. Chemistry

All the reagents were of AR/GR quality and were purchased from Sigma–Aldrich, Loba-Chemie Pt. Ltd., SD Fine Chemicals, Sisco

* Corresponding author. Fax: +91 164 2240555.
  E-mail addresses: raj.khunger@gmail.com, rajcps@cup.ac.in (R. Kumar).
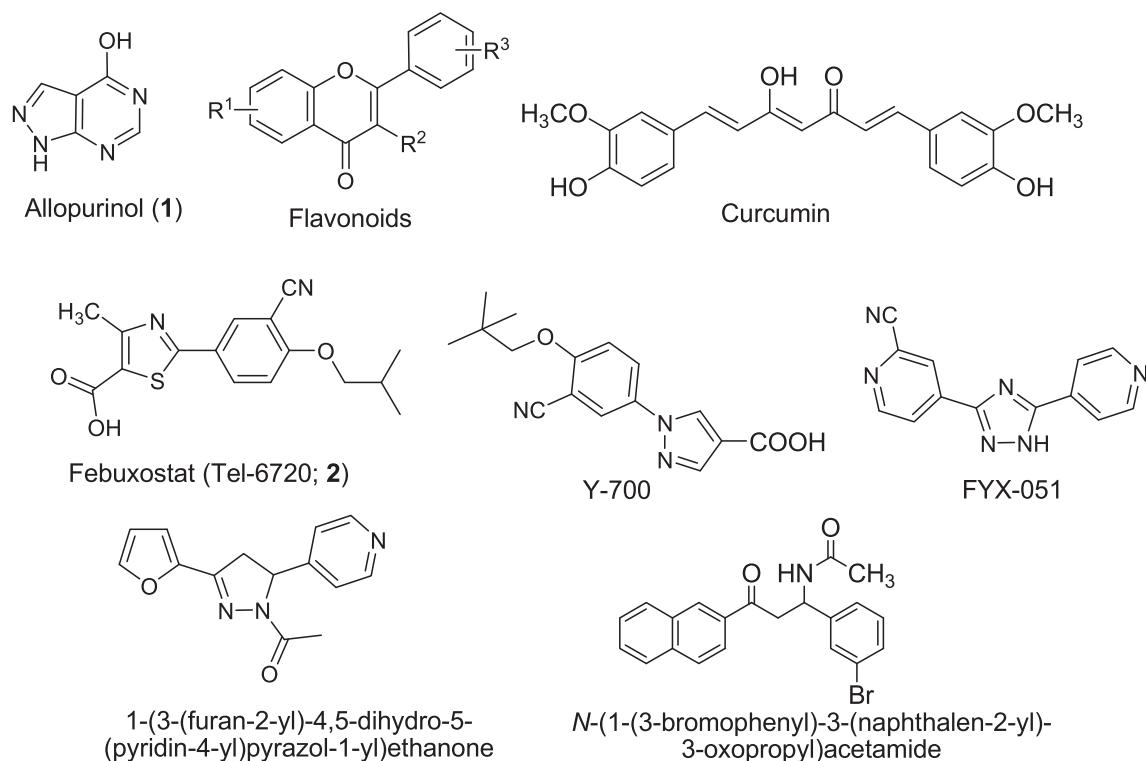[1] CUPB Library Communication Number: P128/14.

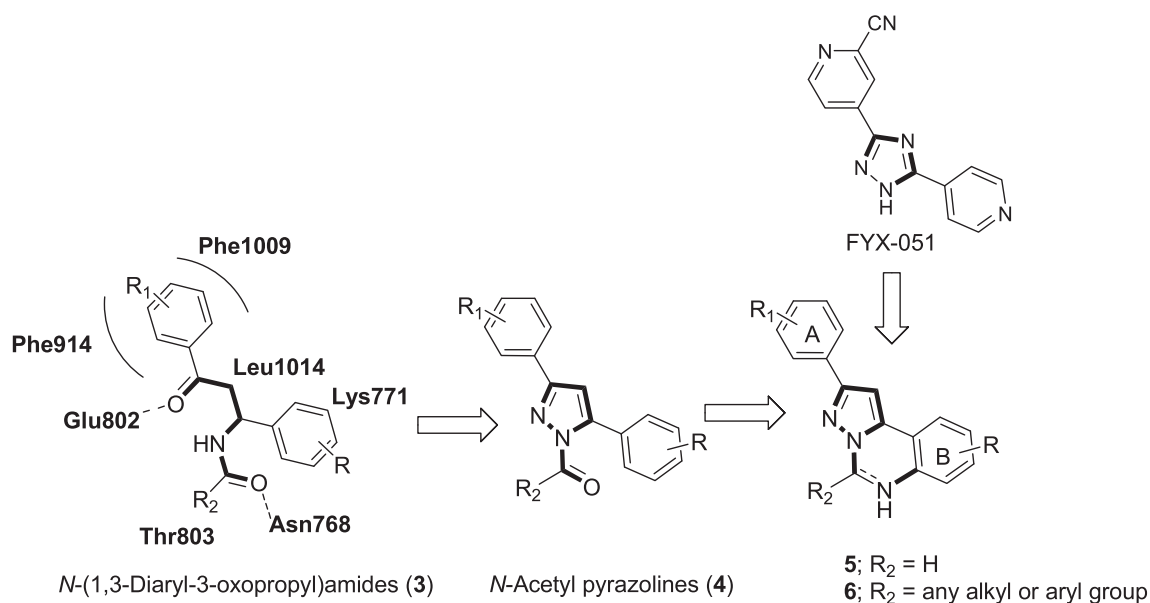**Fig. 1.** Some reported xanthine oxidase inhibitors from our laboratory and others.

Fig. 2. Design of target compounds **5** and **6** as xanthine oxidase inhibitors.

Research Laboratory and HiMedia Laboratories Ltd. and were used without further purification. Sartorius analytical balance (BSA224S-CW) was used for the weighing purposes. JSGW heating mantle, Tarson spinot digital, ILMVAC ROdist digital rotary evaporator, digital hop top and NSW oven/vacuum oven were used during the course of reaction. The progress of the reaction was monitored by TLC, using hexane/ethyl acetate and chloroform/methanol as the mobile phase on pre-coated Merck TLC plates in JSGW UV/fluorescent analysis cabinet and/or iodine chamber. Melting points were recorded on Stuart melting point apparatus (SMP-30) with open glass capillary tubed and was uncorrected.

Infrared (IR) spectra of compounds were recorded with KBr on a Bruker FT-IR spectrophotometer. ^{1}H and ^{13}C Nuclear magnetic resonance (NMR) spectra was obtained in CDCl$_3$/d$_6$-DMSO on a Bruker Avance II (400 MHz) NMR spectrometer using TMS (δ = 0) as internal standard.

2.1.1. Representative procedure for the synthesis of 7

2.1.1.1. *(E)-3-(2-nitrophenyl)-1-phenylprop-2-en-1-one* *(7a)*. A mixture of 2-nitrobenzaldehyde (4 g, 26.50 mmol) and acetophenone (3.18 g, 26.50 mmol) in glacial acetic acid (10 mL) (q.s.) was stirred in 100 mL round bottomed flask (RBF). Conc. Sulfuric acid

(4–5 drops) was added to the reaction mixture in ice cold condition and further stirred at rt for 24 h. After the completion of the reaction (TLC), the reaction mixture was poured on ice cold water and filtered. The solid was washed with water, dried and was recrystallized from methanol to afford the pure compound. Yield: 85%; Creamy white solid; MP: 85–87 °C; IR (KBr, cm^{-1}): 1666 (C=O), 1610 (C=C), 1510 (N=O), 1342 (N=O).

^{1}H NMR (CDCl$_3$, 300 MHz, δ with TMS = 0): 8.12 (1H, d, J = 15.9 Hz), 8.02 (3H, bs), 7.69–7.74 (2H, m), 7.50–7.57 (4H, m), 7.34 (1H, d, J = 15.9 Hz); ^{13}C NMR (CDCl$_3$, 75 MHz, δ with TMS = 0): 190.22, 148.34, 140.03, 137.20, 133.56, 133.09, 131.08, 130.31, 129.13, 128.62, 126.97, 124.86. Similar protocol was utilized for the synthesis of (*E*)-1-(4-chlorophenyl)-3-(2-nitro-phenyl)prop-2-en-1-one (**7b**). The above compounds were used for next steps.

*2.1.1.2. 4,5-Dihydro-5-(2-nitrophenyl)-3-phenyl-1H-pyrazole (**8a**).* A mixture of **7a** (3.3 g, 13.04 mmol) and hydrazine hydrate (0.63 mL, 13.04 mmol) was refluxed under methanol for 2 h. After completion of the reaction (TLC), the reaction mixture was cooled to rt and the precipitates (**8a**) so obtained were collected, dried and used for the next step for further reaction. Yield: 97%; Orange crystalline solid; MP: 140–142 °C; IR (KBr, cm^{-1}): 3310 (N—H), 1518 (N=O), 1333 (N=O), 1299 (C=N); ^{1}H NMR (CDCl$_3$, 400 MHz, δ with TMS = 0): 7.96 (2H, t, J = 8.4 Hz), 7.65 (3H, m), 7.41 (4H, m), 6.05 (D$_2$O exchangeable NH, 1H, s), 5.42 (1H, t, J = 13.2 Hz), 3.80, (1H, q, J = 14.2 Hz), 3.01 (1H, q, J = 13.2 Hz). ^{13}C NMR (CDCl$_3$, 100 MHz, δ with TMS = 0): 151.12, 148.54, 138.04, 133.87, 132.43, 129.06, 128.59, 128.53, 128.36, 126.04, 124.65, 59.83, 41.46. Similar protocol was utilized for the synthesis of 3-(4-chlorophenyl)-5-(2-nitro-phenyl)-4,5-dihydro-1*H*-pyrazole (**8b**).

*2.1.1.3. Synthesis of 5-(2-nitrophenyl)-3-phenyl-1H-pyrazole (**9a**).* **8a** (3.1 g, 11.70 mmol) was refluxed with catalytic amount of molecular iodine in DMSO at 130–140 °C for 2 h. After the completion of reaction (TLC), the reaction mixture was poured in ice cold water and was extracted using ethyl acetate (20 mL × 3). Organics were washed with brine (10 mL × 3), dried over sodium sulfate and evaporated under reduced pressure using rotary evaporator to obtain the product (**9a**) which was used for next step. Yield; 92%; Brownish color solid; MP: 194–196 °C; IR (KBr, cm^{-1}): 3456 (N—H), 1664 (C=N), 1524 & 1348 (N=O), 1217 (C—N); ^{1}H NMR (CDCl$_3$, 400 MHz, δ with TMS = 0): 7.67–7.76 (3H, m), 7.56–7.63 (3H. m), 7.33–7.51 (5H, m); ^{13}C NMR (CDCl$_3$, 100 MHz, δ with TMS = 0): 149.02, 146.37, 146.16, 132.09, 130.97, 129.04, 128.74, 128.04, 126.47, 125.62, 124.56, 123.82, 102.59. Similar protocol was utilized for the synthesis of 5-(2-nitrophenyl)-3-phenyl-1*H*-pyrazole (**9b**).

*2.1.1.4. Representative procedure for the synthesis of 2-(3-Phenyl-1H-pyrazol-5-yl)aniline (**10**).* **9a** (2.75 g, 10.38 mmol) was dissolved in methanol and refluxed with 3 equivalent of stannous chloride dihydrate for 2 h. After the completion of the reaction (TLC), methanol was evaporated under reduced pressure using rotary evaporator followed by neutralization of reaction mixture using 5% NaOH solution. Solid product was than extracted with ethyl acetate (10 mL × 3). Organics were dried over anhydrous sodium sulfate and evaporated under reduced pressure using rotary evaporator to obtain the product **10a** which was used for next step. IR (KBr, cm^{-1}): 3360 (N—H), 3285 (N—H), 1613 (C=N), 1579 (C=C), 1248 (C—N); ^{1}H NMR (CDCl$_3$, 400 MHz, δ with TMS = 0): 13.23 (D$_2$O exchangeable NH, 1H, bs), 7.81 (1H, s), 7.79 (1H, s), 7.31–7.54 (4H, m), 7.00 (2H, s), 6.75 (1H, d, J = 7.91 Hz), 6.61 (1H, t, J = 7.32 Hz), 6.22 (D$_2$O exchangeable NH$_2$, 2H, bs); ^{13}C NMR (CDCl$_3$, 100 MHz, δ with TMS = 0): 149.11, 148.13, 145.37, 133.05, 129.13, 129.10, 128.57, 127.77, 125.14, 119.23, 115.63, 115.29, 99.58. MS

(ESI): *m/z* = 236.1 [M+1]$^+$. All the remaining reactions were carried out using this general procedure [28].

*2.1.1.5. Representative procedure for the synthesis of 2-phenylpyraz-olo[1,5-c]quinazoline (**5a**).* To a solution of **10** (1 mmol, 1.0 equiv) in MeCN (2 mL) was added CH(OEt)$_3$ (1.1 equiv) and was kept in a vial, sealed and put in Biotage Initiator Microwave synthesizer. The reaction mixture was then heated at 100 °C for 10 min (TLC) under MW. After the completion of the reaction, the reaction mixture was left to cool. The precipitates were filtered, dried and washed with *n*-hexane (5 mL × 3) to afford the pure product **5a**. Yield: 91%, Creamy solid: Mp 135–136 °C; IR (KBr, cm^{-1}): 3019 (CH), 1620 (C=N), 1539 (C=C), 1215 (C—N); ^{1}H NMR (DMSO-d$_6$, 600 MHz, δ with TMS = 0): 9.42 (1H, s), 8.30 (1H, d, J = 7.8 Hz), 8.09 (2H, d, J = 8.4 Hz), 7.93 (1H, m), 7.87 (1H, s), 7.75 (2H, m), 7.6 (2H, m), 7.5 (1H, m); ^{13}C NMR (DMSO-d$_6$, 150 MHz, δ with TMS = 0): 155.27, 140.34, 139.96, 139.67, 132.35, 130.57, 129.81, 129.54, 128.85, 128.73, 126.81, 124.21, 119.98, 96.65; MS (ESI): *m/z* = 246 [M+1]$^+$. All the remaining reactions were carried out using this general procedure [28].

*2.1.1.6. Representative procedure for the synthesis of 5-(2,5-dime-thoxyphenyl)-2-phenyl-5,6-dihydropyrazolo [1,5-c]quinazoline (**6a**).* A mixture of **10** (235 mg, 1 mmol, 1.0 equiv) and 2,5-dime-thoxy benzaldehyde (1.0 equiv) in water (2 mL) was taken in a vial, sealed and kept in Biotage Initiator Microwave synthesizer. The reaction mixture was then heated at 100 °C for 15 min (TLC) under MW. After the completion of the reaction, the reaction mixture was left to cool. The precipitates were filtered, dried and washed with *n*-hexane (10 mL × 3) to afford the pure product **6a**. Yield: 80%, Light yellow solid, Mp 230–232 °C; IR (KBr, cm^{-1}): 1644 (C=N), 1587 (C=C), 1220 (C-N), 1123 (C-O); ^{1}H NMR (CDCl$_3$, 400 MHz, δ with TMS = 0): 15.60 (D$_2$O exchangeable NH, 1H, bs), 8.76 (1H, d, J = 8.0 Hz), 8.37 (1H, d, J = 8 Hz), 8.04 (2H, m), 7.55 (2H, d, J = 8.0 Hz), 7.19 (5H, m), 7.11 (3H, m), 7.27 (1H, d, J = 8.27 Hz), 3.70 (3H, s), 3.28 (3H, s); ^{13}C NMR (CDCl$_3$, 100 MHz, δ with TMS = 0): 153.51, 152.15, 149.94, 139.68, 139.25, 133.39, 129.38, 128.60, 127.85, 125.83, 124.06, 123.01, 119.52, 115.31, 113.80, 113.16, 112.70, 111.30, 96.62, 67.99, 56.05, 55.43; HRMS (TOF-ESI) Calcd for C$_{24}$H$_{21}$N$_3$O$_2$, 383.1634 (M)$^+$; observed: 384.1638 (M+H)$^+$. The remaining reactions were carried out using this general procedure [28].

We have recently reported the synthesis and the physical data of **10–10a**, target compounds **5a–5b** and **6b–6m** [28].

2.2. Biological evaluation

Xanthine oxidase enzyme as lyophilized powder was purchased from SRL Pt. Ltd. and stored at temperature below 4 °C. Allopurinol was purchased from SRL Pt. Ltd. Potassium phosphate monobasic (KH$_2$PO$_4$) and dibasic (K$_2$HPO4), DMSO of AR grade were purchased from Loba Chemie Pt. Ltd. Methanol was purchased from SDFCL. Analytical balance (JB1603-c/FACT) and pH meter (Mettler Toledo) were used for the purpose of weighing and measuring the pH, respectively. REMI laboratory refrigerator and ice flaking machine (MSW-136) by Macro scientific works were used for storing solutions. Double-beam UV–Visible spectrophotometer (Shimadzu) for measuring absorbance was used.

2.2.1. Evaluation of XO inhibitory activity
2.2.1.1. Principle of the XO assay. Xanthine oxidase assay is an enzymatic reaction in which xanthine oxidase produces uric acid during oxidation of xanthine. Uric acid can be easily analyzed with an absorption wavelength of 292 nm quantifying xanthine oxidase activity [29].

2.2.1.2. Preparation of reagents.
- Phosphate buffer (50 mM)

For the preparation of 50 mM phosphate buffer at pH 7.5, 9.4 mL (1 M) KH$_2$PO4 (Potassium phosphate monobasic) and 40.6 mL (1 M) K$_2$HPO4 (Potassium phosphate dibasic) was diluted up to 1000 mL with deionised water.

- Xanthine solution (0.10 mM)

Stock solution of 0.1 (M) xanthine was prepared by dissolving 15.2 mg of xanthine in 1 mL of (1 M) NaOH solution. Working solution was made in accordance with 1 μL/mL in deionised water and pH was maintained with 1 N HCl.

- XO enzyme solutions (0.1–0.2 unit/mL)

Stock solution of 16U/mL was prepared by dissolving 1 mg of lyophilised powder of xanthine oxidase enzyme in 1 mL of cold phosphate buffer reagent. For working solution stock solution was diluted up to required volume.

2.2.1.3. Procedure. The inhibitory effect on XO was measured spectrophotometrically at 292 nm under aerobic condition. Allopurinol was used as a positive control for the inhibition test. The reaction mixture consisted of 1.5 mL of 50 mM potassium phosphate buffer (pH 7.5), 1 mL test sample solution (5, 10, 25, 50, and 100 μM) was dissolved in DMSO, 0.5 mL of freshly prepared XO enzyme solution (0.2 units/mL of xanthine oxidase in phosphate buffer). The assay mixture was pre-incubated at room temperature for 15 min. Then, 1 mL of substrate solution (0.10 mM of xanthine) was added into the mixture. The mixture was incubated at room temperature for 30 min. Next, the reaction was stopped with the addition of 1 mL of 1 M HCl. The absorbance was measured using UV–VIS spectrophotometer against a blank prepared in the same way but the xanthine was replaced with the phosphate buffer. Readings were taken in triplicate.

2.2.1.4. Calculation of inhibition. The degree of XO inhibitory activity was calculated by following formula

$$\% \text{ Inhibition} = [(Ac - As)/Ac] \times 100$$

where Ac = Absorbance of control (Sample in absence of XO inhibitors), As = Absorbance of sample (Sample with potential XO inhibitors).

2.2.2. Evaluation of antioxidant activity

Reactive oxygen species can harm various biomolecules including DNA and consequences are oxidative stress in the biological systems. Antioxidants are known to act via reducing the oxidative stress by scavenging of the free radicals and therefore, prevent many diseases including cancer. Hence, we performed DPPH assay to study the antioxidant activity of our compounds *in vitro*. DPPH assay was used to determine the total antioxidant activity by scavenging of the stable DPPH free radical. Antioxidant activity was observed to escalate in the concentration dependent manner [30,31].

2.2.2.1. Principle of DPPH assay. The principle of the assay is the use of the stable free-radical for estimating antioxidant activity 2,2-diphenyl-1-picrylhydrazyl (DPPH) which gets reduced and thus stabilized in presence of a hydrogen donating substance [30].

2.2.2.2. Procedure. 2 mL of the different concentrations of compounds in methanol were added to 2 mL of 0.135 mM methanolic solution of DPPH. The mixture was shaken vigorously and was left to stand for 30 min in the dark. Absorbance was recorded at 517 nm against the blank. Blank was prepared without the addition of DPPH. BHT was used as standard.

2.2.2.3. Calculation of inhibition. The ability to scavenge DPPH radical was calculated by the following equation:

$$\text{DPPH radical scavenging activity}(\%) = [(Ac - As)/Ac] \times 100$$

where Ac = Control (Absorbance of DPPH radical + methanol), As = Sample (Absorbance of DPPH radical + compound).

2.2.3. Molecular docking

The coordinates of the bovine milk XO complexed with salicylic acid were obtained from the protein data bank (PDB entry: 1FIQ) [32]. The ligands were drawn in ChemDraw and subjected to energy minimization via MM2 force field, integrated in Chem3D Ultra. The ligands were docked into the active sites of xanthine oxidase using the Autodock 4.2.5.1, performs Lamarckian genetic algorithm based ligand docking to optimize the conformation of ligand at the receptor binding site. We utilized the grid size $60 \times 60 \times 60$ with a centroid of $26.782 \times 10.121 \times 112.992$ and spacing 0.375. It utilizes energy score fitness function to evaluate the various conformation of ligand at the binding site. This is comprised of various components such as binding energy, ligand efficiency, inhibition constant (μM), inter molecular energy, van der Waals desolvation energy, electrostatic energy, total energy, torsional energy, unbound energy. Each docking experiment was set with 50 different runs with termination after 25,000 energy evaluation. Population size was set out 100. The pose was ranked according to its total energy Score fitness function.
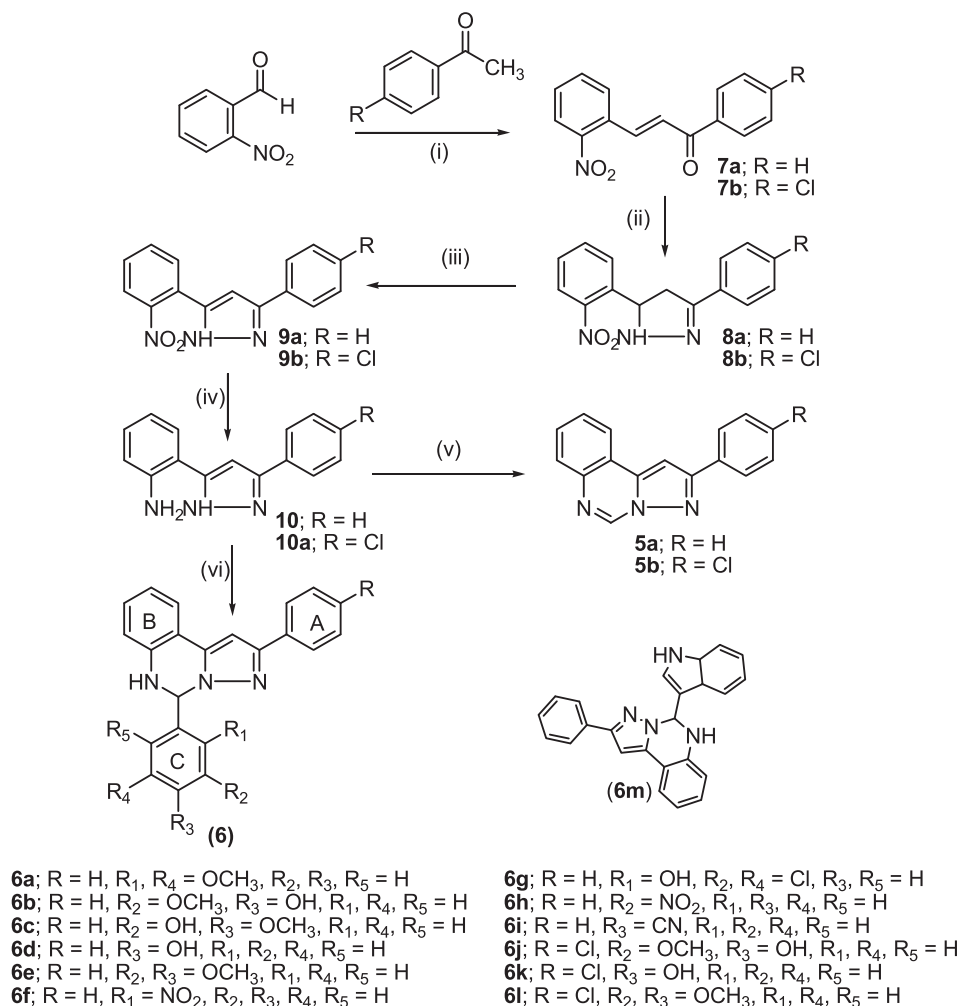
3. Results and discussion

3.1. Chemistry

For the synthesis of target compounds, we followed the route as depicted in Scheme 1. Briefly, the 2-nitrobenzaldehyde was condensed with aryl ketones to afford nitro substituted 1,3-diaryl propenones (**7**) under acid catalyzed conditions. Introduction of pyrazoline ring system (**8**) was made feasible by refluxing **7** with hydrazine hydrate in methanol [33]. The structure of **8** was confirmed by the characteristic ABX pattern with three double doublets in ^{1}H NMR spectrum. Dehydrogenation of **8** to afford pyrazole structure (**9**) was carried out by refluxing with iodine and DMSO [34]. ^{1}H NMR showed the disappearance of ABX pattern due to aromatization and appearance of ^{13}C NMR signal to 100–103 ppm due to C-1 further confirmed the formation of **9**. Reduction of **9** using SnCl$_2$·2H$_2$O in methanol under refluxing afforded **10**. [35] IR spectra confirmed the formation of **10** as a sharp characteristic peak of primary amine (NH$_2$) at 3350–3380 cm^{-1} was obtained. The **10** was eventually cyclocondensed with triethyl orthoformate and different aldehydes under microwave irradiations to yield target compounds **5** and **6**, respectively [28]. A general observation on appearance of chemical shift values in ^{13}C NMR spectra ranging from 66–72 δ and 140–145 δ was noticed for C-5 in case of **6** and **5**, respectively (Fig. 3). All the final products were fully characterized by mp, IR, NMR and HRMS spectral data.

3.2. Biological evaluation

3.2.1. XO inhibitory activity

In order to evaluate the biological activities of synthesized compounds, *in vitro* biochemical screening of the compounds was carried out using xanthine oxidase enzyme with UV–Visible spectrophotometer at 292 nm. Four different concentrations of compounds were used for inhibiting the xanthine oxidase enzyme

6a; R = H, R$_1$, R$_4$ = OCH$_3$, R$_2$, R$_3$, R$_5$ = H
6b; R = H, R$_2$ = OCH$_3$, R$_3$ = OH, R$_1$, R$_4$, R$_5$ = H
6c; R = H, R$_2$ = OH, R$_3$ = OCH$_3$, R$_1$, R$_4$, R$_5$ = H
6d; R = H, R$_3$ = OH, R$_1$, R$_2$, R$_4$, R$_5$ = H
6e; R = H, R$_2$, R$_3$ = OCH$_3$, R$_1$, R$_4$, R$_5$ = H
6f; R = H, R$_1$ = NO$_2$, R$_2$, R$_3$, R$_4$, R$_5$ = H

6g; R = H, R$_1$ = OH, R$_2$, R$_4$ = Cl, R$_3$, R$_5$ = H
6h; R = H, R$_2$ = NO$_2$, R$_1$, R$_3$, R$_4$, R$_5$ = H
6i; R = H, R$_3$ = CN, R$_1$, R$_2$, R$_4$, R$_5$ = H
6j; R = Cl, R$_2$ = OCH$_3$, R$_3$ = OH, R$_1$, R$_4$, R$_5$ = H
6k; R = Cl, R$_3$ = OH, R$_1$, R$_2$, R$_4$, R$_5$ = H
6l; R = Cl, R$_2$, R$_3$ = OCH$_3$, R$_1$, R$_4$, R$_5$ = H

Scheme 1. Reagents and conditions: (i) Acetic acid, H$_2$SO$_4$ (4–5 drops), rt, 24 h; (ii) NH$_2$NH$_2$·2H$_2$O, reflux, 2 h; (iii) I$_2$/DMSO, reflux, 2 h; (iv) SnCl$_2$·2H$_2$O, methanol, reflux, 2 h; (v) CH(OEt)$_3$, acetonitrile, MW, 100 °C, 10–12 min; (f) RCHO, water, MW, 100 °C, 5–15 min.
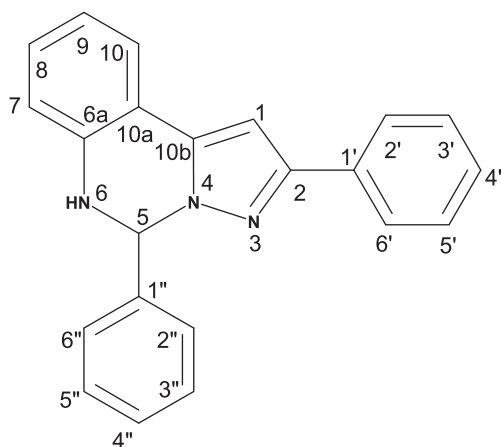
**Fig. 3.** Numbering to the target compounds **5** and **6**.

i.e., uric acid formation as described in experimental section. XO activity i.e. uric acid formation was started by addition of xanthine substrate in different concentration of compounds (5, 10, 25 and 50 μM). The uric acid absorbance was measured spectrophotometrically at 292 nm after an incubation of 30 min. The more potent compounds tend to bind more strongly with XO and decrease the uric acid formation.

All the synthesized target compounds **5a–5b**, **6c–6m** along with the uncyclized compounds **10** and **10a** were tested against the XO enzyme as described in the literature [29] except compounds **6a** and **6c** which were not soluble in the medium under given conditions.

Each compound was tested in triplicate. Among the series compounds tested, **10**, **6b**, **6e**, **6f**, **6g** and **6h** showed significant xanthine oxidase inhibition and reduction in uric acid formation (Fig. 4). Most of the compounds exhibited the good inhibitory potential mainly at concentrations of 25 μM and 50 μM except **6g** which was observed to exhibit the XO inhibitory activity at 5 μM concentration. The compounds that showed the highest *in vitro* XO inhibitory activity are collected in Table 1. Two compounds **6g** and **6h** were found to be most active against XO with IC$_{50s}$ 10.96 μM and 20.89 μM, respectively (Fig. 5 and Table 1) in comparison to allopurinol (IC$_{50}$ = 31.62 μM), standard inhibitor of XO under tested conditions.

3.2.2. Structure activity relationship (SAR)

Some general notions about structure activity relationships emerged from these studies (Fig. 3 and Table 1): (a) uncyclized compounds **10** with no halogen substitution on ring A was found to possess better XO inhibitory activity as compared to **10a**, whereas their products **5a** and **5b**, respectively obtained upon cyclization with CH(OEt)$_3$ were observed to be practically inactive
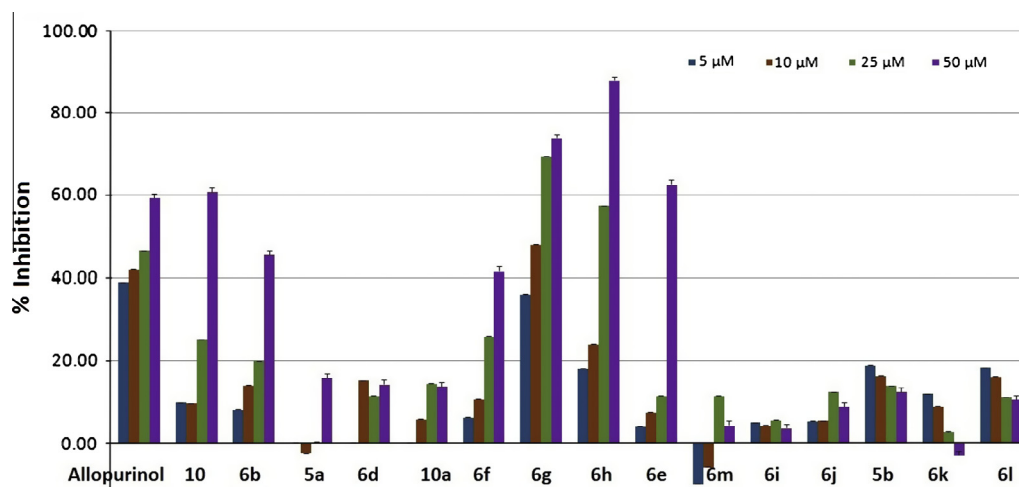
Fig. 4. Percent inhibition of XO with synthesized compounds at concentrations of 5 µM, 10 µM, 25 µM and 50 µM Data is expressed as mean values ± SD of three independent experiments.

Table 1
IC$_{50}$ (half maximal inhibitory concentration) values of some selected compounds.

Compounds	% Inhibition[a]				IC$_{50}$ (µM) xanthine oxidase[b]
	5 µM	10 µM	25 µM	50 µM	
10	9.84	9.63	25.08	60.74	41.69
6b	8.06	13.96	19.86	45.53	ND[c]
6e	4.07	7.39	11.46	62.59	43.65
6g	35.99	47.96	69.38	73.76	**10.96**
6h	17.95	23.98	57.32	87.78	**20.89**
Allopurinol	33.95	42.03	46.53	59.23	31.62

[a] Values are average means of three readings.
[b] Values determined from the midpoint (i.e., 50% inhibition) of the semilog plot.
[c] Not determined.
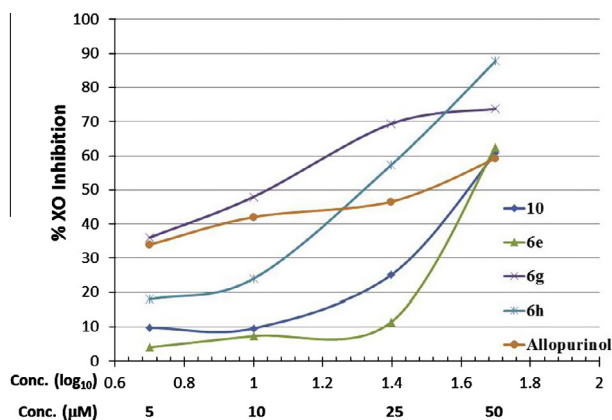
Fig. 5. Semilog plot of concentration vs % inhibition of xanthine oxidase (XO) enzyme. The IC$_{50}$ is identified from the midpoint (i.e., 50% inhibition) of the semilog plot.

against XO, (b) Cyclization of **10** and **10**a with aromatic aldehydes also resulted in decrease or no change in the XO inhibitory activity (compare **10** with **6b**, **6d**, **6e**, **6f** and **6i** and compare **10a** with **6j**, **6k** and **6l**) except in two cases where inhibitory activity was significantly enhanced (compare **10** with **6g** and **6h**), (c) nitro group at *m*-position on Ph at ring C was found to be more tolerable than at *o*-position (compare **6f** with **6h**) whereas not such correlation was noticed in case of activating groups and finally (d) in general, change of Ph on ring C with 3-indolyl resulted in decrease in the

activity (compare **6f**, **6g** and **6h** with **6m**). These observations can be depicted as shown in below:

Rings A and B Ph rings

m-Nitro-Ph > *o*-Nitro-Ph
Ph > 3-indolyl
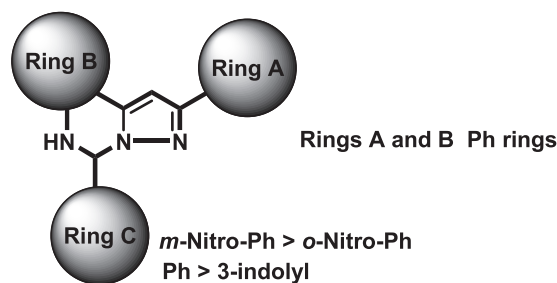
3.2.3. Antioxidant Activity

In order to confirm the antioxidant potential of best XO inhibitory compounds i.e. **6g** and **6h** were tested for their antioxidant potential of which both of them were observed to possess very good antioxidant activity (**6g**, 99% and **6h**, 96%) as they showed significant decrease in the level of DPPH free radical (Table 2). Butylated hydroxyltoluene (BHT) was used as positive control.

3.2.4. Molecular docking

For understanding the recognition process of *R*- and *S*-enantiomers of the most potent identified XO inhibitor **6g** (Fig. 5) docking experiments using Autodock software [36] were performed assuming that it gets accommodated into the salicylic acid XO active site (Fig. 6A) [32]. The docking study showed that *R*-isomer of **6g** (**6gR**) fits well into the XO active site (Fig. 6). The binding mode of **6gR** was found to be similar to those observed in with salicylic acid [32], febuxostat [37] and curcumin [14]. The major interactions of **6gR** with XO include arene/arene interactions with Phe914, Phe1009 and Phe649, three hydrogen bonds with Ser876 and

Table 2
Percentage inhibition of various compounds against DPPH.

S.no.	Compound	Absorbance	% Inhibition
1.	**6g** (4 mM)	0.137	99
2.	**6h** (4 mM)	0.217	96
3.	BHT (5 mM)	0.298	95
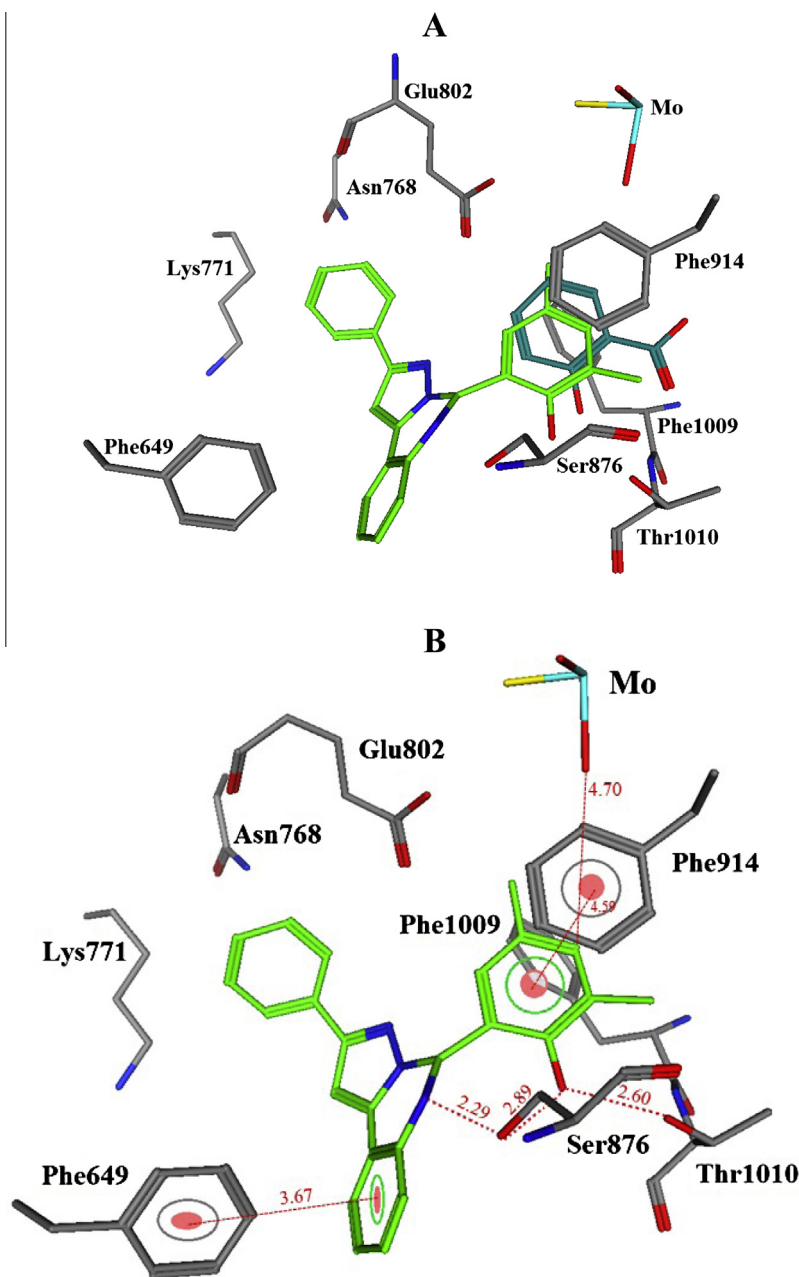
Fig. 6. (A) Docking poses of *R*-isomer of **6g** at the salicylic acid XO binding site (*R*-isomer: green color; salicylic acid: blue color) and, (B) Binding interactions of *R*-isomer of **6g** with the amino acid residues. (For interpretation of the references to color in this figure legend, the reader is referred to the web version of this article.)

Thr1010 (Fig. 6B). The other amino acids such as Glu802, Asn768 and Lys771 also lie in close proximity of the compound. The phenyl rings of Phe914 and Phe1009 lay parallel and perpendicular, respectively to the plane of phenyl ring (ring C) of **6gR** (d = 4.59 Å and d = 3.62 Å). The phenyl residue of Phe649 lies perpendicular to phenyl ring (ring B) of **6gR** (d = 3.67 Å). This kind of arrangement of arene–arene interactions has been previously observed in the co-crystal structures of XO with salicylic acid [32] and febuxostat [37]. This conservation plays an important role in stabilizing the binding positions of aromatic substrates and might well represent one of the key features of the substrate recognition. Three hydrogen bonds, one between N*H* of the inhibitor and free O*H* group of Ser876, second between O*H* of the inhibitor and O*H* of Ser876 and third between O*H* of the inhibitor and O*H* of Thr1010 were observed and provided the rationale for binding of inhibitor.

The ring C of the inhibitor gets positioned towards the dioxoth-iomolybdenum (MOS) moiety at a distance of 4.70 Å indicating that it might block the activity of the enzyme from binding to substrate *via* hydroxylation. The docked conformation of *S*-enantiomer was differing from the *R*-enantiomer. The favorable binding conformation and higher interaction energy of *R*-enantiomer suggests its dominant role in XO inhibitory activity.

4. Conclusions

We have rationally designed, synthesized and evaluated the XO inhibitory activity of some dihydropyrazolo/pyrazolo[1,5-*c*]quinazolines first time. The SAR study disclosed that: (i) nature of rings A, B and C, (ii) nature of substituents on the rings in particular on ring C, and (iii) unsaturation i.e. 5,6-dihydropyrazolo[1,5-*c*]quinazolines were found to affect the XO inhibitory activity. Compound

6g was found to be potent XO inhibitor as compared to allopurinol and capable of scavenge the free radicals in DPPH free radical assay. *In silico* studies highlighted the role of amino acid residues involved in interactions with **6g** and the results are in compliance with the previous reported studies. Further lead optimization on **6g** such as synthesis of compounds with diverse permutation and combinations on ring A, B and C is under progress and will be published in due course

Acknowledgment

References

[1] D. Parks, D. Granger, Acta Physiol. Scand. 548 (1986) 87.
[2] P. Pacher, A. Nivorozhkin, C. Szabo, Pharmacol. Rev. 58 (2006) 87–114.
[3] F. Borges, E. Fernandes, F. Roleira, Curr. Med. Chem. 9 (2002) 195–217.
[4] R. Kumar, Darpan, S. Sharma, R. Singh, Expert Opin. Ther. Pat. 21 (2011) 1071–1108.
[5] H.-Y. Yuan, X.-H. Zhang, X.-L. Zhang, J.-F. Wei, L. Meng, Expert Opin. Ther. Pat. (2014) 1–18.
[6] M. Boban, G. Kocic, S. Radenkovic, R. Pavlovic, T. Cvetkovic, M. Deljanin-Ilic, S. Ilic, M.D. Bobana, B. Djindjic, D. Stojanovic, Ren. Fail. (2014) 1–6.
[7] J. Dawson, M. Walters, Brit. J. Clin. Pharmacol. 62 (2006) 633–644.
[8] J.R. Klinenberg, S.E. Goldfinger, J.E. Seegmiller, Ann. Intern. Med. 62 (1965) 639–647.
[9] J.Z. Singer, S.L. Wallace, Arthritis Rheum. 29 (1986) 82–87.
[10] H. Lee, J. Ariyasinghe, T. Thirumoorthy, Singapore Med. J. 49 (2008) 384.
[11] K. Nepali, A. Agarwal, S. Sapra, V. Mittal, R. Kumar, U.C. Banerjee, M.K. Gupta, N.K. Satti, O.P. Suri, K.L. Dhar, Bioorg. Med. Chem. 19 (2011) 5569–5576.
[12] K. Nepali, G. Singh, A. Turan, A. Agarwal, S. Sapra, R. Kumar, U.C. Banerjee, P.K. Verma, N.K. Satti, M.K. Gupta, Bioorg. Med. Chem. 19 (2011) 1950–1958.
[13] D.W. Kim, M.J. Curtis-Long, H.J. Yuk, Y. Wang, Y.H. Song, S.H. Jeong, K.H. Park, Food Chem. 153 (2014) 20–27.
[14] L. Shen, H.-F. Ji, Bioorg. Med. Chem. Lett. 19 (2009) 5990–5993.
[15] S. Wang, J. Yan, J. Wang, J. Chen, T. Zhang, Y. Zhao, M. Xue, Eur. J. Med. Chem. 45 (2010) 2663–2670.
[16] T. Sato, N. Ashizawa, K. Matsumoto, T. Iwanaga, H. Nakamura, T. Inoue, O. Nagata, Bioorg. Med. Chem. Lett. 19 (2009) 6225–6229.
[17] K.-H. Yu, Recent Pat. Inflammation Allergy Drug Discovery 1 (2007) 69–75.
[18] M.A. Schumacher, H.R. Becker Jr., R.L. Wortmann, P.A. MacDonald, D. Eustace, W.A. Palo, J. Streit, N. Joseph-Ridge, N. Engl. J. Med. 353 (2005) 2450–2461.
[19] H.R. Schumacher, M.A. Becker, R.L. Wortmann, P.A. MacDonald, B. Hunt, J. Streit, C. Lademacher, N. Joseph-Ridge, Arthritis Care Res. 59 (2008) 1540–1548.
[20] Y. Takano, K. Hase-Aoki, H. Horiuchi, L. Zhao, Y. Kasahara, S. Kondo, M.A. Becker, Life Sci. 76 (2005) 1835–1847.
[21] V. Colotta, D. Catarzi, F. Varano, G. Filacchioni, L. Cecchi, A. Galli, C. Costagli, J. Med. Chem. 39 (1996) 2915–2921.
[22] F. Varano, D. Catarzi, V. Colotta, G. Filacchioni, A. Galli, C. Costagli, V. Carlà, J. Med. Chem. 45 (2002) 1035–1044.
[23] F. Varano, D. Catarzi, V. Colotta, F.R. Calabri, O. Lenzi, G. Filacchioni, A. Galli, C. Costagli, F. Deflorian, S. Moro, Bioorg. Med. Chem. 13 (2005) 5536–5549.
[24] F. Beaulieu, C. Ouellet, E.H. Ruediger, M. Belema, Y. Qiu, X. Yang, J. Banville, J.R. Burke, K.R. Gregor, J.F. MacMaster, Bioorg. Med. Chem. Lett. 17 (2007) 1233–1237.
[25] B. Asproni, G. Murineddu, A. Pau, G.A. Pinna, M. Langgard, C.T. Christoffersen, J. Nielsen, J. Kehler, Bioorg. Med. Chem. 19 (2011) 642–649.
[26] F. Varano, D. Catarzi, V. Colotta, O. Lenzi, G. Filacchioni, A. Galli, C. Costagli, Bioorg. Med. Chem. 16 (2008) 2617–2626.
[27] D. Catarzi, V. Colotta, F. Varano, D. Poli, L. Squarcialupi, G. Filacchioni, K. Varani, F. Vincenzi, P.A. Borea, D. Dal Ben, C. Lambertucci, G. Cristalli, Bioorg. Med. Chem. 21 (2013) 283–294.
[28] D. Kumar, R. Kumar, Microwave-assisted synthesis of pyrazolo[1,5-c]quinazolines and their derivatives Tet Lett 55 (2014) 2679–2683.
[29] S.D. Beedkar, C.N. Khobragade, S.S. Chobe, B.S. Dawane, O. Yemul, Int. J. Biol. Macromol. 50 (2012) 947–956.
[30] K.H. Musa, A. Abdullah, B. Kuswandi, M. Amrun Hidayat, Food Chem. 141 (2013) 4102–4106.
[31] M. Szabo, C. Iditoiu, D. Chambre, A. Lupea, Chem. Pap. 61 (2007) 214–216.
[32] C. Enroth, B.T. Eger, K. Okamoto, T. Nishino, T. Nishino, E.F. Pai, Proc. Natl. Acad. Sci. 97 (2000) 10723–10728.
[33] A. Levai, Arkivoc 9 (2005) 344–352.
[34] P. Lokhande, B. Waghamare, S. Sakate, Indian J. Chem., Sect B 44 (2005) 2338.
[35] F. Bellamy, K. Ou, Tet Lett. 25 (1984) 839–842.
[36] X. Jiang, K. Kumar, X. Hu, A. Wallqvist, J. Reifman, Chem. Cent. J. 2 (2008) 1–7.
[37] K. Okamoto, B.T. Eger, T. Nishino, S. Kondo, E.F. Pai, T. Nishino, J. Biol. Chem. 278 (2003) 1848–1855.